Published in final edited form as:
Biomaterials. 2011 March ; 32(9): 2256–2264. doi:10.1016/j.biomaterials.2010.11.065.

Modulus-Driven Differentiation of Marrow Stromal Cells in 3D Scaffolds That Is Independent of Myosin-based Cytoskeletal Tension

Sapun H. Parekh[1,#], **Kaushik Chatterjee**[1,2,#], **Sheng Lin-Gibson**[1], **Nicole M. Moore**[1], **Marcus T. Cicerone**[1], **Marian F. Young**[2], and **Carl G. Simon Jr.**[1,*]

[1]Polymers Division, National Institute of Standards and Technology, Gaithersburg, MD, USA

[2]Craniofacial and Skeletal Diseases Branch, National Institute of Dental and Craniofacial Research, National Institutes of Health, Bethesda, MD, USA

Abstract

Proliferation and differentiation of cells are known to be influenced by the physical properties of the extracellular environment. Previous studies examining biophysics underlying cell response to matrix stiffness utilized a two-dimensional (2D) culture format, which is not representative of the three-dimensional (3D) tissue environment in vivo. We report on the effect of 3D matrix modulus on human bone marrow stromal cell (hBMSC) differentiation. hBMSCs underwent osteogenic differentiation in poly(ethylene glycol) hydrogels of all modulus (300-fold modulus range, from 0.2 kPa to 59 kPa) in the absence of osteogenic differentiation supplements. This osteogenic differentiation was modulus-dependent and was enhanced in stiffer gels. Osteogenesis in these matrices required integrin-protein ligation since osteogenesis was inhibited by soluble Arginine-Glycine-Aspartate-Serine peptide, which blocks integrin receptors. Immunostained images revealed lack of well-defined actin filaments and microtubules in the encapsulated cells. Disruption of mechanosensing elements downstream of integrin-binding that have been identified from 2D culture such as actin filaments, myosin II contraction, and RhoA kinase did not abrogate hBMSC material-driven osteogenic differentiation in 3D. These data show that increased hydrogel modulus enhanced osteogenic differentiation of hBMSCs in 3D scaffolds but that hBMSCs did not use the same mechanosensing pathways that have been identified in 2D culture.

Keywords

three-dimensional culture; bone marrow stromal cell; cytoskeleton; hydrogels; matrix modulus

1. Introduction

Stem cell-based therapeutics have generated great interest as potential treatments for organ replacement and regenerative medicine [1]. Understanding how cells respond to the physical properties of their surroundings is critical to further development of these therapies. Cell function is strongly influenced by the chemical and physical properties of the local

*Corresponding Author: 100 Bureau Drive Gaithersburg MD 20899-8543 301-975-8574 carl.simon@nist.gov.
#These authors contributed equally

extracellular matrix (ECM). Numerous studies have shown that matrix modulus affects cell behaviors such as migration, organization, proliferation and differentiation [2-4], which ultimately play important roles in physiological processes such as organismal development [5] and cancer progression [6, 7].

Human bone marrow stromal cells (hBMSC) are being widely studied as a source of multipotential cells for regenerative medicine [8]. Optimizing the biomaterial modulus is critical for determining hBMSC fates in a tissue scaffold to maximize generation of the desired tissue. Studies have examined the role of modulus in directing cell response using a two-dimensional (2D) culture format [2-4, 6, 7, 9]. It was reported that hBMSCs cultured on low (< 1 kPa), intermediate (8 kPa to 15 kPa), and high (25 kPa to 40 kPa) modulus gels exhibited increased expression of neuronal, myogenic and osteogenic markers, respectively [2]. This study concluded that lineage commitment of hBMSCs could be directed by the substrate modulus alone through a modulus-sensing mechanism mediated by integrin engagement and myosin-based contraction of the actin cytoskeleton.

Subsequently, hBMSC differentiation was shown to be profoundly influenced not only by substrate modulus but also by the ECM protein that was crosslinked onto the substrate [4]. Indeed, mRNA expression of myogenic (MyoD) and osteogenic (Runx2) markers changed significantly when different ECM proteins were crosslinked to gels of the same modulus [4]. In addition to directing cell differentiation, gel modulus was also shown to regulate hBMSC proliferation. Cells on soft gels (250 Pa), similar to the modulus of bone marrow, assumed a quiescent, non-proliferative state while cell proliferation resumed on stiffer gels (7.5 kPa) and was most robust on rigid glass surfaces [3]. Whereas considerable progress has been demonstrated in understanding cellular response to substrate stiffness in 2D formats, the role of matrix modulus in 3D tissue scaffolds is less established. Cellular responses *in vivo* are often different than that observed in planar 2D culture formats, and studies indicate that 3D scaffolds better recapitulate the native tissue environment [10-14]. A recent study has described biophysical mechanisms underlying murine BMSC differentiation in peptide-functionalized hydrogels of different moduli cultured in the presence of both osteogenic and adipogenic supplements. These authors showed that differentiation was regulated by a complex interplay between mechanical and biochemical cues [15].

The objective of the current study was to test the effect of hydrogel modulus on stem cell differentiation in 3D scaffolds and establish the biophysical mechanisms of modulus-driven hBMSC differentiation due to physical cues alone. We describe the response of hBMSCs encapsulated in photopolymerized poly(ethylene glycol) (PEG)-based hydrogels of varying stiffness. PEG hydrogels provide a hydrated environment and are widely used as tissue engineering scaffolds [13, 16]. hBMSCs were encapsulated in PEG hydrogels with compressive moduli varying over a 300-fold range and cultured in growth medium without addition of exogenous biomolecules such as medium supplements (dexamethasone, ascorbic acid, β-glycerophosphate), growth factors, or vectors. Cell differentiation was assayed to investigate the effect of hydrogel modulus on hBMSC fate. Further experiments were performed to identify the mechanostransduction pathway through which hBMSCs interacted with the 3D scaffolds. We used an Arginine-Glycine-Aspartate-Serine (RGDS) peptide that binds to integrin receptors and a series of small molecule inhibitors for actin filaments, microtubules, myosin-mediated contraction, and RhoA kinase (ROCK) to determine if these mechanosensing elements mediated the response of encapsulated hBMSCs to scaffold modulus.

2. Materials and Methods

2.1. Preparation and characterization of scaffolds

4-arm PEG (total relative molecular mass 20000 g/mol, each arm 5000 g/mol, Jemkem Technology) was reacted with 20-fold molar excess of methacrylic anhydride (Sigma-Aldrich) in a consumer microwave for 10 min to prepare PEG- tetramethacrylate (PEGTM) [16]. Hydrogels were prepared by dissolving a known mass fraction of PEGTM (2 %, 3 %, 5 % or 10 %) in 0.1 mol/L phosphate-buffer saline (PBS) containing 0.05 mass % of the photoinitiator Irgacure 2959 (Ciba Chemicals) with 10^6 cells suspended per 1 mL. 50 μL of solution was transferred to Teflon molds (5 mm diameter × 3 mm height) and cured with 365 nm light at 2 mW/cm^2 for 15 min. For mechanical characterization, hydrogels were subjected to a uniaxial static compressive load at a strain rate of 0.03 mm/s by a Dynamic Mechanical Analyzer (TA Instruments). The slope of the linear fit for 5 % to 10 % strain was taken as the measure of the compressive modulus. Shear moduli for the softer gels (2 % and 3 % PEGTM) were measured between parallel plates using a dynamic strain frequency sweep (ARES-LS, TA Instruments). The loss modulus at 10 Hz was used as measure of the shear modulus of the hydrogel.

2.2. Cell culture

Passage 1 human bone marrow stromal cells (hBMSCs) from a 29 year old female donor were obtained from Tulane University Center for Gene Therapy. hBMSCs were characterized by established guidelines for multipotency by the supplier [17]. Medium was prepared from α-modification of Eagle's minimum essential medium containing L-glutamine (α-MEM, Lonza) supplemented with 16 % (volume fraction) fetal bovine serum (Atlanta Biologicals), 2 mmol/L L-glutamine (Sigma-Aldrich), 100 units/mL penicillin and 100 μg/mL streptomycin (Sigma-Aldrich) [18]. Cells from passages 5 and 6 were used for all experiments reported in this study. Control experiments in well plates using osteogenic and adipogenic medium were used to confirm that hBMSCs maintained their multipotency (not shown). For L929 fibroblast (ATCC, CCL-1) control experiments, passage 3 and 4 cells were encapsulated in PEGTM gels and cultured with MEM (Gibco), 10% fetal bovine serum (Gibco), 2 mmol/L L-glutamine (Sigma-Aldrich), and 1 mmol/L sodium pyruvate (Sigma). In all 3D scaffold experiments, cells were encapsulated at 10^6 cells/mL of pre-polymer solution.

For inhibitor studies (all from Sigma), latrunculin A (350 ng/mL), blebbistatin (50 μmol/L), and colchicine (1 μg/mL) were added to the growth medium at each medium change whereas ML-7 (10 μmol/L) and Y-27632 (10 μmol/L) were added to the cultures daily. RGDS peptide (GGGRGDS) was synthesized with an automated peptide synthesizer (APEX 396, Aapptec) using standard solid-phase F-moc chemistry. For RGDS treatments, cells were trypsinized and incubated with RGDS (3.3 mmol/L) for 2 h and RGDS was included in culture medium and refreshed in all medium changes.

2.3. Measurement of cell response

Cell viability was determined semi-quantitatively by staining with calcein AM (Live, 2 μmol/L) and ethidium homodimer-1 (Dead, 2 μmol/L) (Invitrogen) [16]. Resulting live and dead images (3 images per gel) were counted for fractional viability (#live/(#live + #dead). Cells in 0.5 kPa and 59 kPa gels were stained for alkaline phosphatase (following supplier-provided instructions, Sigma-Aldrich) and imaged in whole gels by phase contrast microscopy. Osteocalcin produced by encapsulated hBMSCs was extracted by homogenization of gels [19] and assayed using an enzyme-linked immunosorbent assay (ELISA) against intact human osteocalcin (Biomedical Technologies, BT-460). To quantify the volume of mineral deposited, whole gels were imaged using X-ray micro-computed

tomography [μCT, Scanco μCT 40 , 55 kVp, 145 μA, 10 μm voxel size (isotropic resolution), 0.3 s integration, sigma 1.2, support 2] [16]. Note that 0.2 kPa gels were too soft to handle and reliably image in the μCT system. Calcium deposition in scaffolds was assessed by Alizarin Red S staining of whole gels and imaged by phase contrast microscopy [16]. The chemical composition of the deposited minerals was examined using a one-laser, broadband CARS system [20]. The CARS data is collected as a spectrum (500 cm^{-1} to 3500 cm^{-1}) and processed as described previously [21]. The inset image in Figure 2 is created by plotting the intensity at 952 cm^{-1}.

Cytoskeletal structures were stained [22] and imaged with a Zeiss LSM 510 confocal microscope. Alexa fluor 546 phalloidin (150 nmol/L) and TOPRO-3 (1 μmol/L) (Invitrogen) were added to stain F-actin and DNA. Mouse anti-tubulin primary (2.5 μg/mL) (Sigma, T6074) with FITC anti-mouse IgG secondary (1:200 dilution, Sigma, F5262) were used for imaging microtubules. To stain FN in the gels, mouse anti-FN primary (2.5 μg/mL, Sigma, F7387) and FITC anti-mouse IgG secondary were used followed by TOPRO-3 counterstaining of nuclei.

2.4. Statistical analyses

All data are presented as mean ± S.D. (standard deviation). Statistical analyses were performed by t-test or 1-way ANOVA (analysis of variance) with Tukey's test for multiple comparisons. Differences were considered statistically significant for $p < 0.05$. The "standard deviation" (S.D.) is the same as the "combined standard uncertainty of the mean" for the purposes of this work.

3. Results

3D hydrogels were prepared by photopolymerizing PEGTM polymer solutions containing suspended hBMSCs (Fig. 1A). This process has been extensively used to prepare 3D tissue scaffolds for many different cell types and has been optimized to reduce cytotoxicity [23]. Scaffold compressive modulus increased with increasing PEGTM monomer mass fraction spanning a 300-fold range from 0.2 kPa to 59 kPa for 2 % to 10 % PEGTM, respectively (Fig. 1B). PEGTM solutions with mass fractions less than 2 % did not polymerize and instead formed viscous liquids.

Primary hBMSCs encapsulated in PEGTM gels were cultured growth medium without the addition of differentiation supplements or other biomolecules. Cell viability measured by Live/Dead assay (based on cell membrane integrity and esterase activity) indicated that the fraction of live cells increased marginally with hydrogel modulus (Supplementary Fig. S1A). Previous work has shown that encapsulated cells cannot migrate or proliferate in these non-degradable PEG polymer networks [24].

hBMSC osteogenic differentiation in the hydrogel scaffolds was measured with three independent markers: alkaline phosphatase, calcium phosphate mineral deposition and osteocalcin production. Encapsulation of hBMSCs within 3D PEGTM scaffolds led to a rapid increase in alkaline phosphatase expression within 1 d that was accentuated in stiffer gels (59 kPa) (Fig. 2A). Alkaline phosphatase expression peaked between 1 d and 3 d for both soft (0.5 kPa) and stiff gels (59 kPa), suggesting early onset of osteogenic differentiation.

As a marker for late-stage differentiation, appearance of white deposits in the transparent hydrogels by 14 d qualitatively showed mineral deposition (Fig. 2B). Change in gel appearance from transparent to white scaled with culture time and modulus eventually resulting in an opaque appearance in the stiffest gels (59 kPa) at later time points (42 d) (Fig.

2B). When stained with Alizarin Red S dye for calcium, all gels (0.2 kPa to 59 kPa) stained positive (red) for the presence of minerals by 7 d (Fig. 2C). Red staining increased with stiffness and time such that 59 kPa scaffolds at 42 d were opaque (black) from high density mineral deposits.

Quantification of mineral deposits using X-ray micro-computed tomography (μCT) (Fig. 3A) showed that the mineralized fraction of the scaffolds increased with modulus and was more than 25-fold greater in 59 kPa scaffolds than in softer 0.5 kPa and 11 kPa scaffolds at 42 d. The mineralization in 3D scaffolds was mediated by viable hBMSCs since no minerals (white deposits) were seen in gels without cells (Fig. 2B) or in gels with encapsulated L929 murine fibroblasts which do not possess osteoblastic mineralizing capability (Fig. S1B).

Raman spectra of mineral deposits generated by Coherent anti-Stokes Raman scattering (CARS) microscopy contained a calcium phosphate (952 cm^{-1}) vibrational peak (Fig. 3B), indicating that mineral deposits were calcium phosphate [25]. The calcium phosphate peak was not seen in spectra collected from regions that did not have cells present. hBMSC deposition of minerals caused an increase in modulus of the gels that became significant by 42 d in the 0.5 kPa, 11 kPa, and 59 kPa gels but not in the 0.2 kPa gels (Fig. 1B,C). Previously, control PEG gels incubated without cells showed no change in modulus after 30 d incubations in water [16], showing that these changes in modulus are not influenced by gel degradation over time.

Osteocalcin (OCN), a bone-matrix protein secreted by differentiated osteoblasts, is also a marker for late-stage osteogenesis. OCN in scaffolds increased over time in both soft (0.5 kPa) and stiff gels (59 kPa) (Fig. 3C). Taken together, the alkaline phosphatase, mineral deposition and OCN data demonstrate that encapsulation of hBMSCs in 3D PEG hydrogel scaffolds induced osteogenic differentiation and that stiffer gels drove enhanced differentiation.

Having established that hBMSCs undergo osteogenesis in 3D PEGTM scaffolds, we investigated the intracellular mechanisms driving osteogenic differentiation. Since the PEGTM scaffolds used here were not functionalized with adhesive peptides or ECM proteins that are believed to mediate mechanosensing [26-28], we hypothesized that hBMSCs secreted their own matrix through which they mechanosensed. Indeed, immunostaining detected a 10-fold increase in fibronectin (FN) localized pericellularly around hBMSCs at 7 d in the hydrogels (Fig. 4), indicating that hBMSCs build an ECM within the PEGTM gels. In order to assess if hBMSCs were using the de novo ECM for integrin-based mechanosensing, blocking experiments with soluble RGDS peptides were performed. RGDS moieties are present in ECM proteins and ligate with integrin receptors [28, 29]. Culture of encapsulated hBMSCs in the presence of soluble RGDS inhibited osteogenic differentiation in the gels as shown by Alizarin Red S staining (Fig. 4C) and μCT quantification (Fig. 4D). Live/Dead staining showed that RGDS did not affect hBMSC viability (Supplementary Fig. S2A). These data show that integrin ligation with the de novo ECM was required for hBMSC osteogenesis in PEGTM gels and are consistent with a previous report showing that integrin engagement is required for murine BMSC osteogenesis in RGD-functionalized alginate scaffolds [15].

Previous studies in 2D culture reported that hBMSC morphology and cytoskeletal organization change with substrate modulus concomitant with osteogenic differentiation [2, 3, 30-32]. Enhanced cell spreading with more pronounced actin stress fibers were observed on stiffer substrates relative to soft substrates [30]. In contrast to previous work in 2D, we observed that hBMSCs in the PEGTM gels exhibited a rounded morphology and lacked well-defined actin filaments and microtubules at all moduli and time points (Fig. 5).

Additionally, a spread cell morphology has been shown to promote osteogenic differentiation of hBMSCs [33]. Confining cells to small islands promoted adipogenic differentiation when hBMSCs were cultured in mixed medium with both osteogenic and adipogenic supplements. hBMSCs in the 3D PEGTM scaffolds exhibited osteogenesis (Fig. 2 and 3) and a spherical morphology (Fig. 5) therefore showing no correlation between a spread cell shape and osteogenesis. These data suggest that a rounded cell morphology in 3D scaffolds does not correlate with adipogenic differentiation and are consistent with a recent report showing that hBMSC osteogenesis in 3D RGD-functionalized alginate scaffolds does not correlate with cell spreading [15].

Since hBMSCs synthesized FN and required integrin-ECM protein ligation to induce osteogenic differentiation in scaffolds, it would seem likely that actin filaments, myosin contraction, and ROCK signaling mediated mechanosensitive osteogenesis as shown earlier [2, 15]. Thus, we introduced small molecule inhibitors of actin polymerization (latrunculin A), microtubule formation (colchicine), non-muscle myosin II (blebbistatin), myosin light chain kinase (ML-7), and ROCK (Y-27632) to inhibit osteogenic differentiation of hBMSC in gels (resulting in reduced mineral deposition). Surprisingly, except for latrunculin A, osteogenesis by hBMSCs in gel scaffolds was unaffected by any of the inhibitors as measured by Alizarin Red S staining and by quantification of mineralization by μCT (Fig. 6). Latrunculin A-treatment caused a 2-fold increase in mineral deposition at 14 d compared to untreated controls. These drugs could affect other signaling pathways in addition to their primary target listed above. Thus, Latrunculin-A treatment could have resulted in a significant increase in osteogenesis relative to the untreated control through other pathways. We verified that inhibitors did not affect hBMSC viability as measured by Live/Dead staining (Supplementary Fig. S2A). Cytoskeletal staining revealed that hBMSCs treated with latrunculin A and colchicine had the same rounded morphology as untreated controls (Supplementary Fig. S2B), which was not unexpected based on observations Fig. 5. These data suggest that actin filaments, microtubules, myosin and ROCK are not required for osteogenic differentiation of hBMSCs in non-functionalized PEGTM gels. Previous work with hBMSCs in 2D culture [2, 32, 33] and RGD-functionalized 3D hydrogel scaffolds [15] showed that inhibition of myosin contraction (and tension generation) or disruption of the actin cytoskeleton abrogates stiffness sensing and osteogenic differentiation, which is inconsistent with the data presented here.

4. Discussion

Our results show that hBMSCs spontaneously committed to an osteogenic lineage, without differentiation supplements, that was enhanced by increasing matrix stiffness when encapsulated into 3D PEGTM scaffolds (Fig. 2 and 3). By using a soluble RGDS peptide, we show that integrin-ECM interactions were required for hBMSC osteogenic differentiation in 3D (Fig. 4), consistent with previous work [15]. However, using small molecule inhibitors to disrupt cytoskeletal structure and myosin/ROCK tension generation, it was observed that acto-myosin mediated contraction was not required for osteogenic differentiation (Fig. 6) in contrast to previous 2D [2, 34] or 3D work using RGD-functionalized scaffolds [15].

In recent work, Huebsch *et al.* showed that both hBMSCs and murine BMSCs (mBMSCs) cultured in the presence of mixed adipogenic and osteogenic supplements can be driven toward either adipogenic or osteogenic differentiation based on 3D hydrogel stiffness [15]. In the current work, hBMSCs cultured without differentiation supplements underwent 3D osteogenic differentiation at all moduli tested, but stiffer gels enhanced osteogenic differentiation. Obvious differences between the two studies are species and supplements. The current human work (hBMSCs) may differ from the Huebsch *et al.* mouse work

(mBMSCs) since there may be functional differences in BMSCs from the two species that influence how they differentiate. For instance, different mixes of supplements are required to induce mBSMC [15] versus hBMSC differentiation [35]. Importantly, the mBMSC differentiation measured by Huebsch *et al.* was a result of a combination of mechanical (gel modulus) and biochemical cues (mixed soluble supplements) whereas the present work measured the effect of mechanical cues alone (no differentiation supplements were used). In addition, PEG gels used in our study were not bio-functionalized with RGD unlike the work of Huebsch *et al.*, and studies have indicated that availability and concentration of biomolecules can affect cellular response to matrix modulus [4, 36]. It is likely that different cell signaling pathways are involved in the two conditions. For example, hBMSCs in non-functionalized PEG scaffolds may use intermediate filaments to mechanosense as has been shown for shear flow-enhanced cyclooxygenase (COX)-2 expression in pre-osteoblast cells [37].

A common finding of our work and that of Huebsch *et al.* is the integrin-dependence of modulus-driven 3D differentiation. Huebsch *et al.* used RGD-functionalized scaffolds to actively engage integrin receptors and ligation of α_5-integrin with RGD was necessary for osteogenic differentiation in 3D. In the current work, hBMSCs initially encountered a non-functionalized scaffold but synthesized a FN-containing matrix over time. Addition of soluble RGDS peptide to block integrin-ECM engagement prevented hBMSC osteogenic differentiation indicating that mechanosensing in 3D gels was mediated via integrin binding. Taken together, these data suggest that while integrin-ECM protein binding is necessary for purely modulus-driven osteogenesis in 3D scaffolds, the downstream pathway is independent of the myosin II-based contractile machinery and microtubules, perhaps highlighting a role for intermediate filaments as mechanosensing elements. As mentioned above, recent reports have implicated intermediate filaments as a possible mechanosensor. These filaments are organized at focal adhesions and have been shown to associate with integrin molecules intracellularly [38]. Disruption of intermediate filaments leads to changes in cell shape [39] and cell response to stress [40]. Therefore, it is possible that mechanostransduction in 3D scaffolds flows from integrin-ECM ligation through intermediate filaments as has been described recently [41].

In summary, it is becoming evident that cell fate in 3D scaffolds is determined by both physical and biochemical cues through complex intracellular signaling pathways. It is likely that different cue combinations may lead to similar outcomes, with an optimum parameter space still to be determined [42]. These studies have important implications for rational design of 3D tissue scaffolds for regenerative medicine applications by showing that material properties influence cell signaling in unique ways.

5. Conclusions

This study examined the effect of matrix modulus on hBMSC fate in 3D PEG hydrogel scaffolds. Encapsulation of hBMSCs induced osteogenic differentiation over the full range of modulus (0.2 kPa to 59 kPa) studied here in the absence of exogenous biomolecules. Osteogenesis was sensitive to gel modulus and maximal differentiation was observed in the stiffest gels (59 kPa). Integrin engagement with the extracellular matrix proteins synthesized de novo was critical to scaffold-induced osteogenesis. In contrast to established biophysical pathways in 2D culture, hBMSC differentiation in 3D hydrogels did not involve actin filaments and microtubules along with myosin-mediated contraction and RhoA kinase (ROCK) activity. These experiments demonstrate that other cell-signaling pathways are involved in 3D.

Supplementary Material

Refer to Web version on PubMed Central for supplementary material.

Acknowledgments

K.C., S.H.P., and N.M.M. were supported by Research Associateship Awards from the National Research Council of the National Academy of Sciences. This work was supported by NIST, NIH-NIBIB R21 EB006497-01 and the Intramural Program of the NIH-NIDCR. The Tulane Center for Gene Therapy provided hBMSCs (NCRR/NIH P40RR017447). The content is solely the responsibility of the authors and does not necessarily represent the official views of NIH or NIST. Certain equipment and instruments or materials are identified in the paper to adequately specify the experimental details. Such identification does not imply recommendation by NIST, nor does it imply the materials are necessarily the best available for the purpose.

References

[1]. Barry FP, Murphy JM. Mesenchymal stem cells: clinical applications and biological characterization. Int J Biochem Cell B. 2004; 36(4):568–84.

[2]. Engler AJ, Sen S, Sweeney HL, Discher DE. Matrix elasticity directs stem cell lineage specification. Cell. 2006; 126(4):677–89. [PubMed: 16923388]

[3]. Winer JP, Janmey PA, McCormick ME, Funaki M. Bone marrow-derived human mesenchymal stem cells become quiescent on soft substrates but remain responsive to chemical or mechanical stimuli. Tissue Eng Part A. 2009; 15(1):147–54. [PubMed: 18673086]

[4]. Rowlands AS, George PA, Cooper-White JJ. Directing osteogenic and myogenic differentiation of MSCs: interplay of stiffness and adhesive ligand presentation. Am J Physiol Cell Physiol. 2008; 295(4):1037–44.

[5]. Zhou JA, Kim HY, Wang JHC, Davidson LA. Macroscopic stiffening of embryonic tissues via microtubules, RhoGEF and the assembly of contractile bundles of actomyosin. Development. 2010; 137(16):2785–94. [PubMed: 20630946]

[6]. Paszek MJ, Zahir N, Johnson KR, Lakins JN, Rozenberg GI, Gefen A, et al. Tensional homeostasis and the malignant phenotype. Cancer Cell. 2005; 8(3):241–54. [PubMed: 16169468]

[7]. Ulrich TA, Pardo EMD, Kumar S. The mechanical rigidity of the extracellular matrix regulates the structure, motility, and proliferation of glioma cells. Cancer Res. 2009; 69(10):4167–74. [PubMed: 19435897]

[8]. Bianco P, Robey PG, Simmons PJ. Mesenchymal stem cells: Revisiting history, concepts, and assays. Cell Stem Cell. 2008; 2(4):313–19. [PubMed: 18397751]

[9]. Fu JP, Wang YK, Yang MT, Desai RA, Yu XA, Liu ZJ, et al. Mechanical regulation of cell function with geometrically modulated elastomeric substrates. Nat Methods. 2010; 7(9):733–36. [PubMed: 20676108]

[10]. Petersen OW, Ronnovjessen L, Howlett AR, Bissell MJ. Interaction with basement-membrane serves to rapidly distinguish growth and differentiation pattern of normal and malignant human breast epithelial-cells. Proc Natl Acad Sci U S A. 1992; 89(19):9064–68. [PubMed: 1384042]

[11]. Doyle AD, Wang FW, Matsumoto K, Yamada KM. One-dimensional topography underlies three-dimensional fibrillar cell migration. J Cell Biol. 2009; 184(4):481–90. [PubMed: 19221195]

[12]. Lammermann T, Bader BL, Monkley SJ, Worbs T, Wedlich-Soldner R, Hirsch K, et al. Rapid leukocyte migration by integrin-independent flowing and squeezing. Nature. 2008; 453(7191): 51–55. [PubMed: 18451854]

[13]. Peyton SR, Kim PD, Ghajar CM, Seliktar D, Putnam AJ. The effects of matrix stiffness and RhoA on the phenotypic plasticity of smooth muscle cells in a 3-D biosynthetic hydrogel system. Biomaterials. 2008; 29(17):2597–07. [PubMed: 18342366]

[14]. Cukierman E, Pankov R, Stevens DR, Yamada KM. Taking cell-matrix adhesions to the third dimension. Science. 2001; 294(5547):1708–12. [PubMed: 11721053]

[15]. Huebsch N, Arany PR, Mao AS, Shvartsman D, Ali OA, Bencherif SA, et al. Harnessing traction-mediated manipulation of the cell/matrix interface to control stem-cell fate. Nat Mater. 2010; 9:518–26. [PubMed: 20418863]

[16]. Chatterjee K, Lin-Gibson S, Wallace WE, Parekh SH, Lee YJ, Cicerone MT, et al. The effect of 3D hydrogel scaffold modulus on osteoblast differentiation and mineralization revealed by combinatorial screening. Biomaterials. 2010; 31(19):5051–62. [PubMed: 20378163]

[17]. Dominici M, Le Blanc K, Mueller I, Slaper-Cortenbach I, Marini F, Krause D, et al. Minimal criteria for defining multipotent mesenchymal stromal cells. The International Society for Cellular Therapy position statement. Cytotherapy. 2006; 8(4):315–17. [PubMed: 16923606]

[18]. Block GJ, Ohkouchi S, Fung F, Frenkel J, Gregory C, Pochampally R, et al. Multipotent stromal cells are activated to reduce apoptosis in part by upregulation and secretion of stanniocalcin-1. Stem Cells. 2009; 27(3):670–81. [PubMed: 19267325]

[19]. Hauschka PV, Frenkel J, Demuth R, Gundberg CM. Presence of osteocalcin and related higher molecular-weight 4-carboxyglutamic acid-containing proteins in developing bone. J Biol Chem. 1983; 258(1):176–82. [PubMed: 6600233]

[20]. Lee YJ, Parekh SH, Kim YH, Cicerone MT. Optimized continuum from a photonic crystal fiber for broadband time-resolved coherent anti-Stokes Raman scattering. Opt Express. 2010; 18(5): 4371–79. [PubMed: 20389449]

[21]. Liu Y, Lee YJ, Cicerone MT. Broadband CARS spectral phase retrieval using a time-domain Kramers-Kronig transform. Opt Lett. 2009; 34(9):1363–65. [PubMed: 19412273]

[22]. Thibault MM, Buschmann MD. Migration of bone marrow stromal cells in 3D: 4 color methodology reveals spatially and temporally coordinated events. Cell Motil Cytoskel. 2006; 63(12):725–40.

[23]. Williams CG, Malik AN, Kim TK, Manson PN, Elisseeff JH. Variable cytocompatibility of six cell lines with photoinitiators used for polymerizing hydrogels and cell encapsulation. Biomaterials. 2005; 26(11):1211–18. [PubMed: 15475050]

[24]. Kloxin AM, Kasko AM, Salinas CN, Anseth KS. Photodegradable hydrogels for dynamic tuning of physical and chemical properties. Science. 2009; 324(5923):59–63. [PubMed: 19342581]

[25]. Sauer GR, Zunic WB, Durig JR, Wuthier RE. Fourier-transform Raman-spectroscopy of synthetic and biological calcium phosphates. Calcified Tissue Int. 1994; 54(5):414–20.

[26]. Wozniak MA, Chen CS. Mechanotransduction in development: a growing role for contractility. Nat Rev Mol Cell Bio. 2009; 10(1):34–43. [PubMed: 19197330]

[27]. Katsumi A, Orr AW, Tzima E, Schwartz MA. Integrins in mechanotransduction. J Biol Chem. 2004; 279(13):12001–4. [PubMed: 14960578]

[28]. Hynes RO. Integrins: bidirectional, allosteric signaling machines. Cell. 2002; 110(6):673–87. [PubMed: 12297042]

[29]. Byron A, Humphries JD, Askari JA, Craig SE, Mould AP, Humphries MJ. Anti-integrin monoclonal antibodies. J Cell Sci. 2009; 122(22):4009–11. [PubMed: 19910492]

[30]. Yeung T, Georges PC, Flanagan LA, Marg B, Ortiz M, Funaki M, et al. Effects of substrate stiffness on cell morphology, cytoskeletal structure, and adhesion. Cell Motil Cytoskel. 2005; 60(1):24–34.

[31]. Discher DE, Janmey P, Wang YL. Tissue cells feel and respond to the stiffness of their substrate. Science. 2005; 310(5751):1139–43. [PubMed: 16293750]

[32]. Khatiwala CB, Peyton SR, Putnam AJ. Intrinsic mechanical properties of the extracellular matrix affect the behavior of pre-osteoblastic MC3T3-E1 cells. Am J Physiol Cell Physiol. 2006; 290(6):C1640–50. [PubMed: 16407416]

[33]. McBeath R, Pirone DM, Nelson CM, Bhadriraju K, Chen CS. Cell shape, cytoskeletal tension, and RhoA regulate stem cell lineage commitment. Dev Cell. 2004; 6(4):483–95. [PubMed: 15068789]

[34]. Ruiz SA, Chen CS. Emergence of patterned stem cell differentiation within multicellular structures. Stem Cells. 2008; 26(11):2921–27. [PubMed: 18703661]

[35]. Sekiya I, Larson BL, Vuoristo JT, Cui JG, Prockop DJ. Adipogenic differentiation of human adult stem cells from bone marrow stroma (MSCs). J Bone Miner Res. 2004; 19(2):256–64. [PubMed: 14969395]

[36]. Wall ST, Yeh C-C, Tu RYK, Mann MJ, Healy KE. Biomimetic matrices for myocardial stabilization and stem cell transplantation. J Biomed Mater Res A. 2010; 95A(4):1055–66. [PubMed: 20878934]

[37]. Norvell SM, Ponik SM, Bowen DK, Gerard R, Pavalko FM. Fluid shear stress induction of COX-2 protein and prostaglandin release in cultured MC3T3-E1 osteoblasts does not require intact microfilaments or microtubules. J Appl Physiol. 2004; 96(3):957–66. [PubMed: 14617531]

[38]. Homan SM, Martinez R, Benware A, LaFlamme SE. Regulation of the association of alpha 6 beta 4 with vimentin intermediate filaments in endothelial cells. Exp Cell Res. 2002; 281(1):107–14. [PubMed: 12441134]

[39]. Goldman RD, Khuon S, Chou YH, Opal P, Steinert PM. The function of intermediate filaments in cell shape and cytoskeletal integrity. J Cell Biol. 1996; 134(4):971–83. [PubMed: 8769421]

[40]. Pekny M, Lane EB. Intermediate filaments and stress. Exp Cell Res. 2007; 313(10):2244–54. [PubMed: 17524394]

[41]. Wang N, Tytell JD, Ingber DE. Mechanotransduction at a distance: mechanically coupling the extracellular matrix with the nucleus. Nat Rev Mol Cell Bio. 2009; 10(1):75–82. [PubMed: 19197334]

[42]. Kelly DJ, Jacobs CR. The role of mechanical signals in regulating chondrogenesis and osteogenesis of mesenchymal stem cells. Birth Defects Res C-Emb Tod-Rev. 2010; 90(1):75–85.

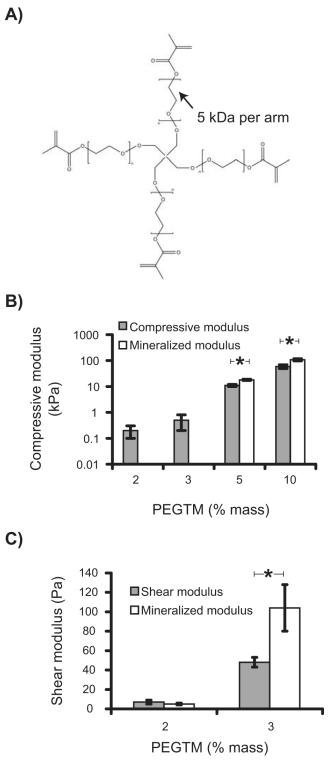

Figure 1.

(A) Chemical structure of the PEGTM monomer with four methacrylate end-groups that facilitate formation of the hydrogel by chemical crosslinking. **(B)** Plot of compressive modulus of hydrogels for different mass fractions of PEGTM. **(C)** Softer gels (2 % and 3 % PEGTM) were characterized in shear modulus as well due to their lower compressive modulus. Graphs also show compressive **(B)** and shear **(C)** moduli of mineralized scaffolds at 42 d culture with hBMSCs. Statistical differences ($p < 0.05$, t-test, $n = 4$) are indicated by asterisk.

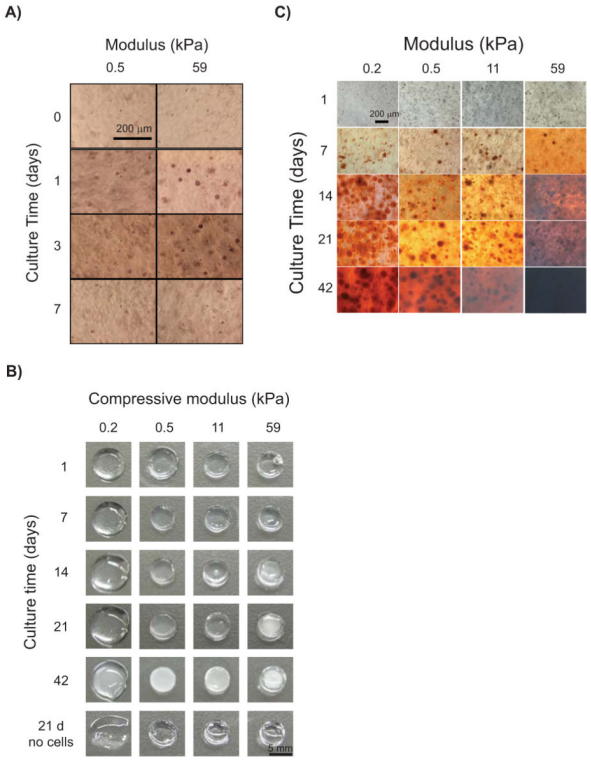

Figure 2.

hBMSC osteogenic differentiation in 3D PEGTM scaffolds increased with compressive modulus. **(A)** Alkaline phosphatase staining of hBMSCs at 0 d, 1 d, 3 d, and 7 d showed enzyme production peaked by 3 d in both 0.5 kPa and 59 kPa scaffolds, indicating early osteogenic differentiation. **(B)** Representative photographs of hydrogel scaffolds showing that mineralization by hBMSCs in PEGTM scaffolds increased with time and modulus. Mineral desposition in the gels caused a change in appearance from transparent to white. Control scaffolds without cells appeared transparent at 21 d, confirming that mineralization is a specific response from hBMSC osteogenic differentiation in the scaffolds. **(C)** Alizarin Red S staining demonstrated calcium deposition in all scaffolds by hBMSCs by 7 d and staining became more intense with time and modulus.

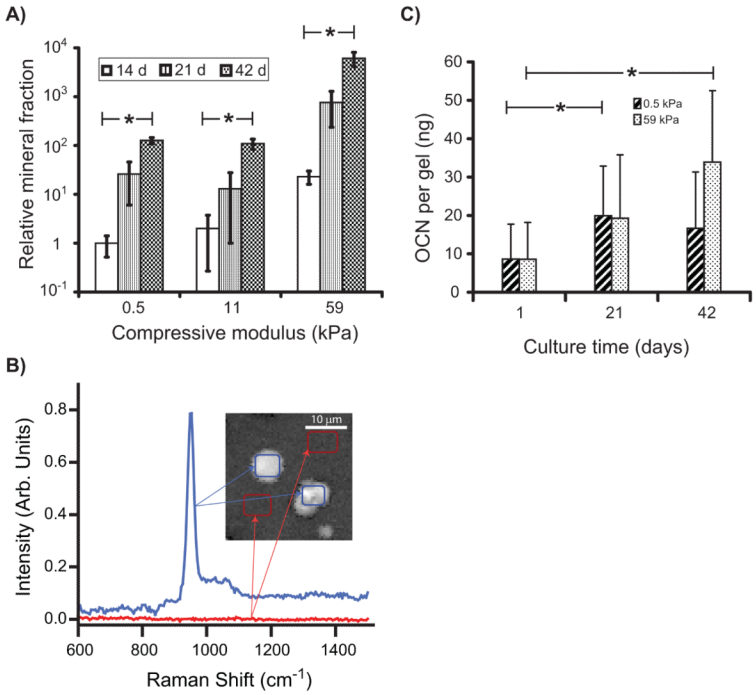

Figure 3.

Quantitative analysis of osteogenic differentiation in 3D PEG scaffolds. **(A)** μCT analysis of mineral deposits demonstrated that the mineralized volume fraction in all scaffolds increased with modulus and time. All mineralized fractions were normalized to the mineral volume measured in 0.5 kPa gels at 14 d (n = 3). **(B)** Chemical imaging by CARS microscopy of 59 kPa gels containing hBMSCs cultured for 21 days. CARS identified a characteristic phosphate peak at 952 cm^{-1} that corresponded to a (phosphate) resonance found in amorphous calcium phosphate (blue trace). Areas of the gel without cells (red trace) showed no peaks. *(Inset)* CARS image built from the 952 cm^{-1} where white indicates areas rich in calcium phosphate in the scaffold. Spectra from the blue and red regions of the image were used to generate the corresponding traces in plot. **(C)** Osteocalcin (OCN) produced by hBMSCs increased with time in both soft and stiff scaffolds over time measured by ELISA (n = 4). Statistical differences ($p < 0.05$, 1-way ANOVA with Tukey's) are indicated with asterisk.

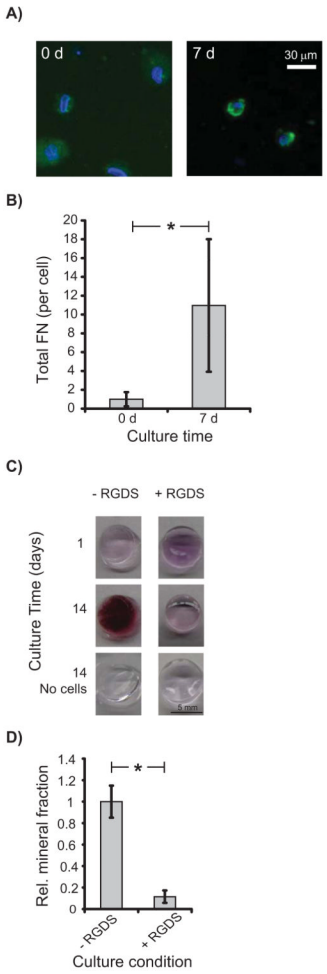

Figure 4.

hBMSCs in 11 kPa PEGTM scaffolds synthesized FN and RGDS peptide blocked osteogenesis. **(A)** Little FN was detected by antibody staining in hydrogels cultured 0 d with hBMSCs. However, gels at 7 d demonstrated FN deposits as shown by the bright green pericellular fluorescence. Cell nuclei and FN were blue and green, respectively. **(B)** Total pericellular FN per hBMSC increased 10-fold from 0 d (n = 25 cells) to 7 d (n = 16 cells). FN images were identically thresholded for 0 d and 7 d to mark the FN area around nuclei, and normalized FN pixel values (by the background fluorescence) were integrated over this area. The graph showed total FN per cell relative to 0 d. **(C)** Alizarin Red S staining of hBMSCs cultured with RGDS peptide reduced mineralization. Mineralization was inhibited in scaffolds cultured with RGDS compared to scaffolds cultured without RGDS. **(D)** Scaffolds treated with RGDS peptide exhibited decreased mineralization at 14 d as measured by μCT (n = 3). Statistical difference ($p < 0.05$, 1-way ANOVA with Tukey's) is indicated by asterisk.

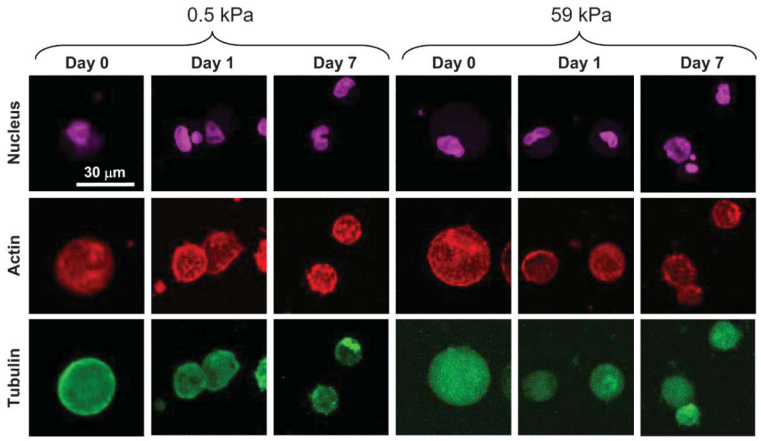

Figure 5.

Maximum intensity projections of confocal image stacks of hBMSCs in 3D PEGTM scaffolds of 0.5 kPa and 59 kPa. F-actin (red), tubulin (green) and nuclear (purple) staining showed that cells maintained a rounded morphology independent of scaffold modulus. hBMSCs in both soft and stiff scaffolds did not exhibit well-defined actin or microtubule structures.

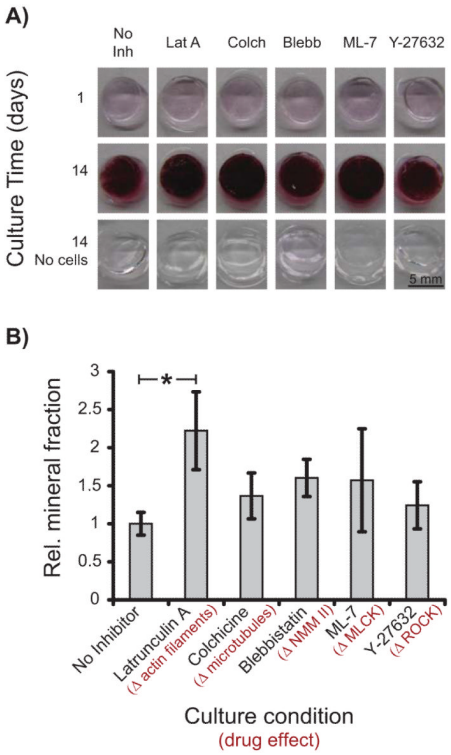

Figure 6.

Cytoskeletal integrity was not required for osteogenic differentiation in 3D PEGTM scaffolds. **(A)** Alizarin Red S staining of hBMSCs in 11 kPa scaffolds treated with inhibitors of actin polymerization, microtubule formation, myosin contraction, and ROCK inhibitors revealed that hBMSCs underwent osteogenesis regardless of cytoskeletal inhibition. **(B)** Quantification of mineralized volume with μCT showed that inhibitors did not block hBMSC osteogenesis at 14 d(n = 3). Statistical differences ($p < 0.05$, 1-way ANOVA with Tukey's) are indicated by asterisk.